

PLANETARY SCIENCE

A heterogeneous mantle and crustal structure formed during the early differentiation of Mars

James M. D. Day^{1*}, Marine Paquet^{1,2}, Arya Udry³, Frederic Moynier⁴

Highly siderophile element abundances and Os isotopes of nakhlite and chassignite meteorites demonstrate that they represent a comagmatic suite from Mars. Nakhlites experienced variable assimilation of >2-billion-year-old altered high Re/Os basaltic crust. This basaltic crust is distinct from the ancient crust represented by meteorites Allan Hills 84001 or impact-contaminated Northwest Africa 7034/7533. Nakhlites and chassignites that did not experience crustal assimilation reveal that they were extracted from a depleted lithospheric mantle distinct from the deep plume source of depleted shergottites. The comagmatic origin for nakhlites and chassignites demonstrates a layered martian interior comprising ancient enriched basaltic crust derived from trace element-rich shallow magma ocean cumulates, a variably metasomatized mantle lithosphere, and a trace element-depleted deep mantle sampled by plume magmatism.

INTRODUCTION

Meteorites from Mars provide fundamental insights into the evolution of what was once a potentially habitable planet. As dominantly basaltic rocks ranging in age from >4.4 billion years (Ga) to <0.2 Ga (1–4), martian meteorites have been used to demonstrate much earlier completion of accretion and core formation for Mars than Earth (5), evidence that Mars was once completely molten and likely had a magma ocean (6), early oxidation of the crust through impacts (7), and evidence for liquid water and alteration processes at the surface [e.g., (8–10)]. In the absence of returned samples from Mars' surface, meteorites are essential to understanding the petrogenesis of distinct rock types [e.g., (1, 4, 11, 12)] and are crucial for geochemical and geophysical models.

Of the available martian meteorites, two distinctive rock types, the augite-rich basaltic nakhlites (12) and the olivine-rich dunitic chassignites (13), have been postulated to represent a comagmatic suite [e.g., (14)]. As likely representatives of a single magmatic system, they have similar crystallization (1.34 ± 0.04 Ga) and ejection ages from the martian surface (11 ± 1.5 million years) (14, 15) and so have the potential to provide unparalleled information on magmatic processes within Mars. These rocks have been interpreted to have formed from a relatively long-lived magmatic system (15), with a depleted source composition, suggesting that they are relatively low-degree partial melt products generated from flexural uplift of metasomatized mantle lithosphere, possibly within the Tharsis region of Mars (16).

In contrast to a comagmatic origin, it has been suggested that nakhlites and chassignites may not be related (17), and it remains unclear how other martian meteorite types, including shergottites, the orthopyroxenite Allan Hills (ALH) 84001 (18), or the basaltic breccia Northwest Africa (NWA) 7034/7533 [and pairs; (3, 19)], relate to this igneous suite. To resolve these issues, we present Re-Os isotope and highly siderophile element (HSE; Os, Ir, Ru, Pt, Pd, and Re) abundance data for chemically well-characterized nakhlites and chassignites, expanding previous work (20–23). In turn, this enables determination of

whether nakhlites and chassignites are related and insights into their petrogenetic histories. In addition, we report Re-Os isotope and HSE abundance data for the orthopyroxenite ALH 84001 to examine the likely nature of ancient crustal rocks on Mars to complement studies on the ~4.4-Ga basaltic breccia NWA 7034/7533 (24).

RESULTS

Sample powders analyzed for ^{187}Re - ^{187}Os and HSE abundances have been previously measured for major and trace element abundances (16, 25) or are reported here (ALH 84001 and Y-000802). Nakhlites are basaltic rocks with low total alkalis (<2 wt % $\text{Na}_2\text{O} + \text{K}_2\text{O}$; fig. S1), span a range of MgO (7.3 to 12.3 wt %) and Cr (496 to 2305 $\mu\text{g/g}$) contents (fig. S2), and, as noted previously (14, 16), have consistent Chondrite Ivuna (CI)-normalized incompatible trace element (ITE) patterns (fig. S3). Chassignites are dunites with low total alkalis (<0.2 wt % $\text{Na}_2\text{O} + \text{K}_2\text{O}$), 32 to 36 wt % MgO, and high Cr (4700 to 10,400 $\mu\text{g/g}$) and have overlapping ITE patterns with nakhlites. In contrast, the ancient martian sample ALH 84001 [4.1 Ga; (2)] is an orthopyroxenite with ~24 wt % MgO, high Cr (7700 $\mu\text{g/g}$), and an ITE pattern most similar to shergottite meteorites but with elevated high field strength element abundances (fig. S3). Nakhlites and chassignites have compatible element abundance variations consistent with olivine (+clinopyroxene) and Cr-spinel fractionation or accumulation, respectively, while ALH 84001 is an accumulative rock containing dominantly orthopyroxene and Cr-spinel (fig. S2).

The HSE abundance and Os isotope compositions of nakhlites, chassignites, and ALH 84001 are given in table S1 and Figs. 1 and 2. Nakhlite fractions examined in this study have variable total HSE abundances (0.65 to 10.2 ng/g), $^{187}\text{Re}/^{188}\text{Os}$ (0.4 to 61), and measured $^{187}\text{Os}/^{188}\text{Os}$ (0.164 to 1.369) ratios. Martian mantle normalized HSE patterns for the nakhlite suite (Fig. 1) are similar to fractionated terrestrial alkali basalt partial melts (26), with high $(\text{Re} + \text{Pd} + \text{Pt})/(\text{Ru} + \text{Ir} + \text{Os})$ ratios. Age-corrected $^{187}\text{Os}/^{188}\text{Os}$ range from unrealistically low to high γ_{Os_i} (–111 to +306), where γ_{Os_i} is the percentage deviation in $^{187}\text{Os}/^{188}\text{Os}$ relative to a chondritic reference calculated for 1.34 Ga (14). Some nakhlites, including most fractions of Nakhla, conform to a 1.34-Ga chondritic initial isochron, whereas others plot at higher $^{187}\text{Os}/^{188}\text{Os}$ for a given $^{187}\text{Re}/^{188}\text{Os}$ ratio, consistent with more radiogenic initial Os (Fig. 2).

Analyzed chassignites have relatively low total HSE abundances (2.4 to 4.1 ng/g) compared with some nakhlites and previously published data for chassignites or nakhlites (20–23), having low $^{187}\text{Re}/^{188}\text{Os}$ (0.11

Copyright © 2024 The Authors, some rights reserved; exclusive licensee American Association for the Advancement of Science. No claim to original U.S. Government Works. Distributed under a Creative Commons Attribution NonCommercial License 4.0 (CC BY-NC).

¹Scripps Institution of Oceanography, University of California San Diego, La Jolla, CA 92093, USA. ²Centre de Recherches Péetrographiques et Géochimiques de Nancy, CNRS, Université de Lorraine 15 Rue Notre Dame des Pauvres 54500 Vandoeuvre-lès-Nancy, France. ³Department of Geoscience, University of Nevada, Las Vegas, Lilly Fong Geoscience Building, 4505 S Maryland Pkwy, Las Vegas, NV 89154, USA. ⁴Université Paris Cité, Institut de Physique du Globe de Paris, CNRS, 1 rue Jussieu, 75005 Paris, France.

*Corresponding author. Email: jmday@ucsd.edu

to 0.21) and sub-chondritic $^{187}\text{Os}/^{188}\text{Os}$ (0.1177 to 0.1231). Martian mantle normalized HSE patterns are generally relatively flat for chassignite fractions (Fig. 1) and are similar to terrestrial cumulate dunites (27). Age-corrected $^{187}\text{Os}/^{188}\text{Os}$ are close to chondritic ($\gamma\text{Os}_i = -5$ to $+2$), with generally invariant $^{187}\text{Os}/^{188}\text{Os}$ for a range of $^{187}\text{Re}/^{188}\text{Os}$ (Fig. 2). Sample ALH 84001 has low total HSE abundances (0.23 to 0.84 ng/g), $^{187}\text{Re}/^{188}\text{Os}$ from 5.4 to 74, and measured $^{187}\text{Os}/^{188}\text{Os}$ broadly within the range of chondrites (0.1237 to 0.1299). Martian mantle normalized HSE patterns are strongly fractionated for ALH 84001, with negative age-corrected $^{187}\text{Os}/^{188}\text{Os}$, indicating recent rhenium disturbance.

DISCUSSION

Comagmatic origin for nakhlites and chassignites

The nakhlites, chassignites, and ALH 84001 represent meteorites obtained as either falls (e.g., Nakhla and Chassigny) or finds (e.g., Lafayette), including those from the Antarctic (e.g., ALH 84001) or from hot deserts (NWA designated samples). No systematic trends

are discernable for the HSE or Os isotopes based on these distinctions, implying that terrestrial alteration effects have had negligible influence on these elemental and isotopic characteristics. The only exceptions are disturbance to Re contents in some samples, with extremely negative calculated γOs_i (table S1). This disturbance is unrelated to neutron fluence effects, as hypothesized for some lunar samples with long cosmic-ray exposure histories (28), given the relatively limited exposure ages for martian meteorites [e.g., (4)]. Instead, they more likely reflect Re disturbance or, in some cases, large blank subtraction on Re [e.g., (29)]. These effects have limited impact on measured $^{187}\text{Os}/^{188}\text{Os}$ or overall HSE abundance patterns.

The new HSE data for nakhlites and chassignites are fundamental to considering their potential comagmatic origins. Nakhlites and chassignites are closely related in terms of ejection and crystallization ages and ITE and Sr-Nd isotope compositions (14, 16, 30), yet their relationship to one another has been questioned [e.g., (17, 31)]. A comagmatic origin is supported by fractionation of olivine and Cr-spinel to form cumulate chassignites and fractionated nakhlite compositions, indicating a mineral assemblage with between ~98 and 94% olivine (and clinopyroxene) and ~2 and 6% Cr-spinel (fig. S2). Fractionation processes are modeled in three steps for the

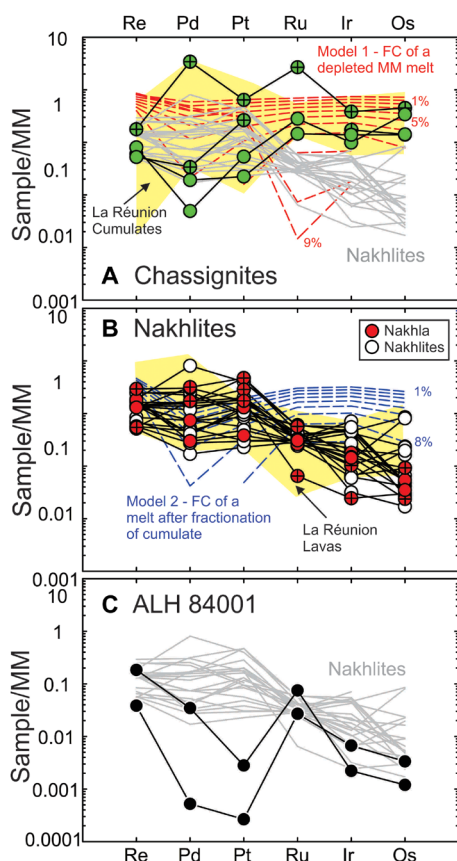


Fig. 1. Martian mantle normalized HSE patterns. Shown in (A) are chassignites, (B) nakhlites, and (C) ALH 84001. Symbols with crosses denote previously published data. Shown in (A) is model 1, a fractional crystallization (FC) model of a depleted martian mantle (MM) composition that experienced 5% prior melt depletion. Partial melt depletion of the MM composition results in only minor depletions of most HSE to the residue, with more major depletion for Pd, due to the lack of S exhaustion at these relatively low melt fractions. Shown in (B) is model 2, a fractional crystallization model for a melt after dunite (chassignite) cumulate removal. Model information is provided in the methods and the MM composition is from (32). Field of La Réunion cumulate dunites and lavas from (27). Published chassignite and nakhlite data from (20–23).

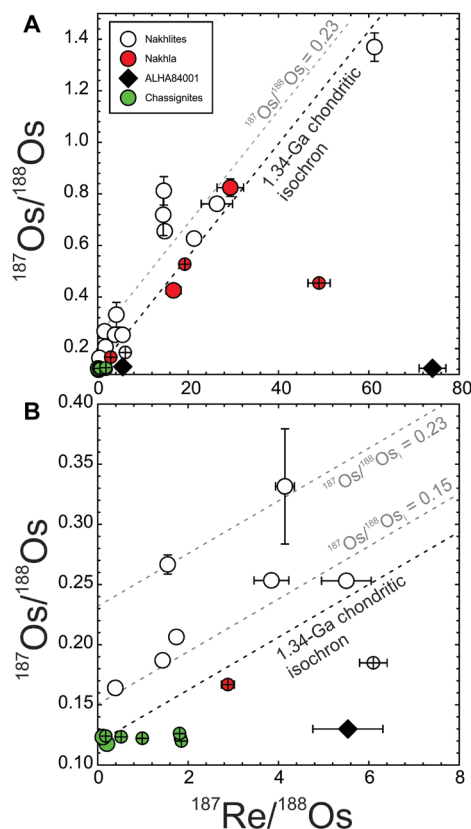


Fig. 2. Rhenium-osmium isotope diagrams for nakhlites, chassignites, and ALH 84001. (A) The full range of ^{187}Re - ^{187}Os in the samples. (B) An expanded view of the lower left-hand region of (A). Symbols with crosses denote previously published data. The nakhlite meteorite Nakhla is separated from other nakhlites in these diagrams, as different sample fragments have been measured in this study and (20–23). Shown for reference are the 1.34-Ga chondritic reference isochron and 1.34-Ga isochrons with radiogenic initial $^{187}\text{Os}/^{188}\text{Os}$ of 0.15 and 0.23. Published data from (20, 22, 23).

HSE. First, given the requirement for a depleted mantle source for both meteorite classes in Mars (16), a previously fertile mantle source (32) that experienced ~5% prior melt depletion was modeled. This process acted to marginally reduce the HSE contents of the source relative to the martian mantle estimate due to S remaining in the mantle residue (Fig. 1A). In the second stage, the depleted mantle source experienced variable extents of partial melt depletion and was assumed to accumulate minerals to form chassignites (Fig. 1A). In the third stage, the residual liquid after dunite cumulate removal (chassignite) was further fractionated, assuming a mineral assemblage dominated by olivine [clinopyroxene would have a similar effect, given that the empirically derived partition coefficients between both phases are not substantially different; (26)], Cr-spinel, and sulfide (Fig. 1B).

The more fractionated patterns of nakhlites compared with chassignites match similar trends for terrestrial dunite cumulates and lavas from La Réunion and can be modeled through crystal-liquid fractionation effects (Fig. 1). This is further supported by the correspondence of chondritic initial $^{187}\text{Os}/^{188}\text{Os}$ of many nakhlites with chassignite compositions (Fig. 2), indicating a mantle-derived primary melt composition. To form both chassignites and nakhlites, the primary mantle melt would have to have been MgO-rich [11 to 13 wt %; e.g., (33)], to model the sample compositions, rather than MgO-poor from parental melt estimates from nakhlite melt inclusion studies [e.g., (34–36)]. Melt inclusions within nakhlite clinopyroxene and olivine are, therefore, representative of late-stage liquids after prior fractional crystallization. The MgO-rich nature of the parent melt required to explain the relatively flat HSE patterns of chassignites suggests ~5% partial melting of their mantle source.

Crustal assimilation occurring in nakhlites

A large fraction of the studied nakhlites have a high $^{187}\text{Os}/^{188}\text{Os}$ for a given $^{187}\text{Re}/^{188}\text{Os}$ ratio, evident in them falling along the more radiogenic initial isochron lines illustrated in Fig. 2. While this feature could reflect Re disturbance, or blank corrections, as noted previously, the measured $^{187}\text{Os}/^{188}\text{Os}$ for nakhlites is extreme and requires substantial initial magmatically derived variations in Re/Os as well as initial isotopic heterogeneity. Because some nakhlites have similar chondritic initial $^{187}\text{Os}/^{188}\text{Os}$ to chassignites, the most likely explanation for initial Os isotopic heterogeneity would be through assimilation of high Re/Os crustal material, during nakhlite emplacement, concomitant with fractional crystallization.

The HSE are chalcophile in the absence of metal (37) and so are strongly controlled by sulfide in martian magmas (38). Studies of nakhlite and ALH 84001 sulfur isotope compositions have demonstrated that they span a range of $\delta^{34}\text{S}$, as well as of the mass-independent signature $\Delta^{33}\text{S}$, which has been attributed to assimilation of surface sulfate formed through photochemical effects in Mars' atmosphere (9, 39, 40). The compositional range of S isotopes implies alteration by fluids in equilibrium with the martian atmosphere to the ancient basaltic crust. This crust was then assimilated into some nakhlites. Measured $^{187}\text{Os}/^{188}\text{Os}$ and S isotope data from different aliquots of samples have a negative covariation (Fig. 3); the only exception is the meteorite Nakhla, which has $\Delta^{33}\text{S}$ close to zero (no anomaly) and a range of $^{187}\text{Os}/^{188}\text{Os}$ within different aliquots. ALH 84001 also lacks a large $\Delta^{33}\text{S}$ anomaly and had low Re/Os, implying that it is not a good representative of a likely assimilant for nakhlites. Instead, the assimilant had negative $\Delta^{33}\text{S}$ and high Re/Os. This altered basaltic crust was likely also Cl-rich to explain the compositions of some

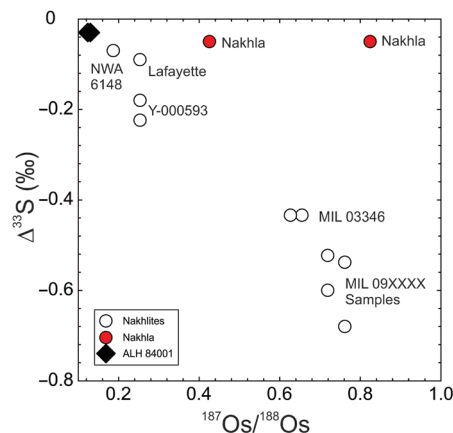


Fig. 3. Measured $^{187}\text{Os}/^{188}\text{Os}$ versus $\Delta^{33}\text{S}$ for nakhlites and ALH 84001. Sulfur isotope data are from different aliquots to Os measured in this study from (9, 39, 40). Plots of age-corrected $^{187}\text{Os}/^{188}\text{Os}$ versus $\Delta^{33}\text{S}$ reveal the same negative correlation but with more scatter due to the disturbance of Re in some of the studied meteorites (see the "Crustal assimilation occurring in nakhlites" section for details). MIL 09XXXX refers to MIL 090030, MIL 090032, and MIL 090136.

nakhlites (30). A notable feature of the Os-S isotope covariation is that poorly equilibrated nakhlites, which have vitrophyric matrices and large ranges in pyroxene composition [MIL designated meteorites; (41, 42)] have the most radiogenic measured $^{187}\text{Os}/^{188}\text{Os}$ and negative $\Delta^{33}\text{S}$ relative to the more equilibrated nakhlites with crystal-line matrix [Lafayette and Nakhla; (14)]. Such a relationship implies that some fast-quenched nakhlites experienced more considerable assimilation of high-Re/Os and altered martian crust.

To constrain the nature of the assimilant responsible for the variations of Os and S isotope and trace element compositions within nakhlites, mixing models were constructed between a mantle melt responsible for chassignites and nakhlites with two likely crustal compositions (Fig. 4). The first is an enriched shergottite [Los Angeles; (43)] composition with high $^{187}\text{Os}/^{188}\text{Os}$. While this sample is considerably younger than nakhlites or chassignites and so cannot be a realistic assimilant, it illustrates that an enriched shergottite-type composition is a likely crustal contaminant composition for nakhlites and chassignites in Mars. The second composition was produced by taking enriched shergottite compositions and aging them for Os isotopes to the oldest known shergottites at ~2.4 Ga (44, 45). This operation was done to provide an estimate of ingrowth of ^{187}Os from ^{187}Re decay in potential realistically aged basaltic assimilants to the nakhlites. A potential source that can be ruled out is impact-contaminated ancient basaltic crust, such as that represented by NWA 7034/7533 (24), which would not match the radiogenic $^{187}\text{Os}/^{188}\text{Os}$ of contaminated nakhlites. While all shergottites have lower La/Yb than nakhlites or chassignites, depleted shergottites are not a match for a possible crustal source composition because they do not have sufficiently high Re/Os to generate large $^{187}\text{Os}/^{188}\text{Os}$ variations over time. Instead, our models illustrate that <10% assimilation of an ancient (>2 Ga) altered basaltic crustal composition, similar in composition to enriched shergottites, occurred to explain the compositional variability of nakhlites (Fig. 4). Substantial fractional crystallization (e.g., Fig. 1) concomitant with assimilation to produce nakhlite parental melt compositions would be consistent with these estimates, suggesting that assimilation may have occurred in

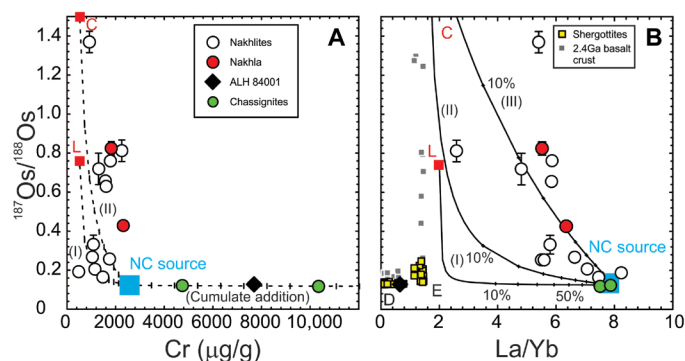


Fig. 4. Modeling assimilation and fractional crystallization processes in nakhlites and chassignites. Only data from this study are shown for nakhlites and chassignites as powder aliquots have been measured for both $^{187}\text{Os}/^{188}\text{Os}$ as well as (A) Cr and (B) La/Yb. Models in (A) and (B) show mixing between a nakhlite-chassignite primary mantle melt (NC source, blue square; Cr, 2500 $\mu\text{g/g}$; Os, 1.5 ng/g; $^{187}\text{Os}/^{188}\text{Os}$, ~ 0.125 ; La/Yb, 8; and La, 3.8 $\mu\text{g/g}$) and a Los Angeles composition (II) L; Cr, 600 $\mu\text{g/g}$; Os, 0.004 ng/g; $^{187}\text{Os}/^{188}\text{Os}$, ~ 0.74 ; La/Yb, 2; and La, 2 $\mu\text{g/g}$) and a hypothetical ~ 2.4 -Ga high-Re/Os crustal component (C; Cr, 500 $\mu\text{g/g}$; $^{187}\text{Os}/^{188}\text{Os}$, ~ 2 ; La/Yb, 1.6; and La, 1 $\mu\text{g/g}$), with ratios of Os contents of either 75 relative to the NC source (III); Os, 0.02 ng/g) or 15 (III); 0.1 ng/g) to illustrate the influence of Os content in the partial melt produced from the assimilant. The Os isotopic composition of the 2.4-Ga crustal component represents the predicted ingrowth of ^{187}Os from enriched shergottite samples, shown by the gray squares in (B). Also shown is the effect of cumulate addition between the NC source to an olivine cumulate with Cr-spinel (Cr, $>20,000$ $\mu\text{g/g}$; and Os, >3 ng/g). The Los Angeles composition is from (43), with other shergottite data from (16) and (32). The notations of D and E show the composition of ~ 0.2 Ga to 0.6 Ga depleted and enriched basaltic shergottites, respectively.

shallow sills where partial melting enhanced ITE enrichment from assimilating wall rocks.

A heterogeneous martian mantle and crustal structure

Observations of a comagmatic origin for chassignites and nakhlites, with the latter experiencing variable assimilation of altered enriched basaltic crust during emplacement, have implications for understanding links between martian meteorites and the magmatic evolution of Mars. Contamination from old altered enriched basaltic crust without evidence for HSE enrichment from impact provides constraints regarding the crust into which nakhlites and chassignites were emplaced. Evidence in support of ancient enriched basaltic crustal components is provided from alkali basalt-type compositions determined by the Mars Exploration Rovers (MER) (fig. S1). These basalt compositions have been obtained from relatively young impact contamination-poor Amazonian surfaces on Mars, consistent with a Tharsis origin (16). We suggest that the alkalic tendencies of basalts measured by the MER reflect partial melting of enriched lithospheric components from pervasive metasomatism or from direct melting of shallow incompatible element enriched magma ocean cumulates in Mars (Fig. 5). The younger enriched shergottites are also likely to be derived from these sources, with a major implication being that depleted shergottites are derived from deeply derived mantle sources sampled by plumes. In turn, ALH 84001 is a deep- to mid-crustal cumulate from dominantly enriched basaltic crust in Mars, with impact-ejected rocks (NWA 7034) likely to reflect materials from the older, more cratered southern hemisphere of Mars (Fig. 5).

As a comagmatic suite, nakhlites and chassignites provide crucial information on martian magmatic processes, indicating similarities with alkali basalt magmatism on Earth (46). Furthermore, assimilation into some nakhlite meteorites enables unambiguous identification of relatively ancient (>2 Ga) high Re/Os, incompatible element enriched basaltic crust that has interacted with the atmosphere. Martian magmas are strongly influenced by relatively shallow mantle (e.g., nakhlites and chassignites, and enriched shergottites) and deeper plume derived partial melting processes (depleted shergottites) and this structure can potentially be examined by geophysical models from the Insight mission and from future Mars sample return.

MATERIALS AND METHODS

Sample descriptions and sources

Analyses were conducted on powders made from chips of samples from various sources (table S4). This included separately sourced chips of the Nakhla meteorite. Chips were unpacked from the original containers that they were received from and were examined with the naked eye to check for exterior fusion crust. Only material without fusion crust was crushed, in a pre-cleaned alumina mortar and pestle. The resultant ~ 1 to 2 g powder aliquots were used for major and trace element abundance determination (14, 16, 32) followed by Re-Os isotope and HSE abundance analysis. In some instances, discrete analyses of sample powders were conducted to assess replication and the effect of nuggetting of the HSE in samples.

Major and trace element abundance determinations and sources

New major and trace element abundance data are reported for nakhlite Y-000802 and ALH 84001 (table S2). The data were obtained in an identical way to previously reported data by our group on nakhlites and chassignites [e.g., (14, 16, 25, 32)] at the Scripps Isotope Geochemistry Laboratory (SIGL). This included digestion of a 50-mg aliquot from a larger mass of sample powder (1 to 2 g) also used for Re-Os isotope and HSE abundance analysis. Complete digestion was accomplished by sealing sample with Teflon-distilled 27.5 M HF (4 ml) and 15.7 M HNO_3 (1 ml) in closed-capped Teflon beakers for >72 hours on a hotplate at 150°C , along with total procedural blanks and terrestrial basalt and andesite reference materials (BHVO-2, BCR-2, BIR-1a, and AGV-2). Samples were sequentially dried and taken up in concentrated HNO_3 to destroy fluorides, followed by doping with indium to monitor instrumental drift during analysis, and then diluted to a factor of 5000. Trace element abundances were determined using a Thermo Fisher Scientific iCAP Qc quadrupole inductively coupled plasma mass spectrometer (ICP-MS), and all data are blank-corrected. Long-term reproducibility of abundance data is better than 6% for most elements, except for Mo, Te, and Se ($>10\%$).

Osmium isotope and HSE (Re, Pd, Pt, Ru, Ir, and Os) abundances

Osmium isotope and HSE abundance analyses were performed at the SIGL on precisely weighed aliquots of homogenized powder that were then digested in 10-cm sealed borosilicate Carius tubes with isotopically enriched multielement spikes (^{99}Ru , ^{106}Pd , ^{185}Re , ^{190}Os , ^{191}Ir , and ^{194}Pt) and 7 ml of a 1:2 mixture of multiply Teflon distilled HCl and HNO_3 purged of excess Os by repeated treatment and reaction with H_2O_2 . Samples were digested to a maximum temperature of 270°C in an oven for 72 hours. Osmium was triply extracted from

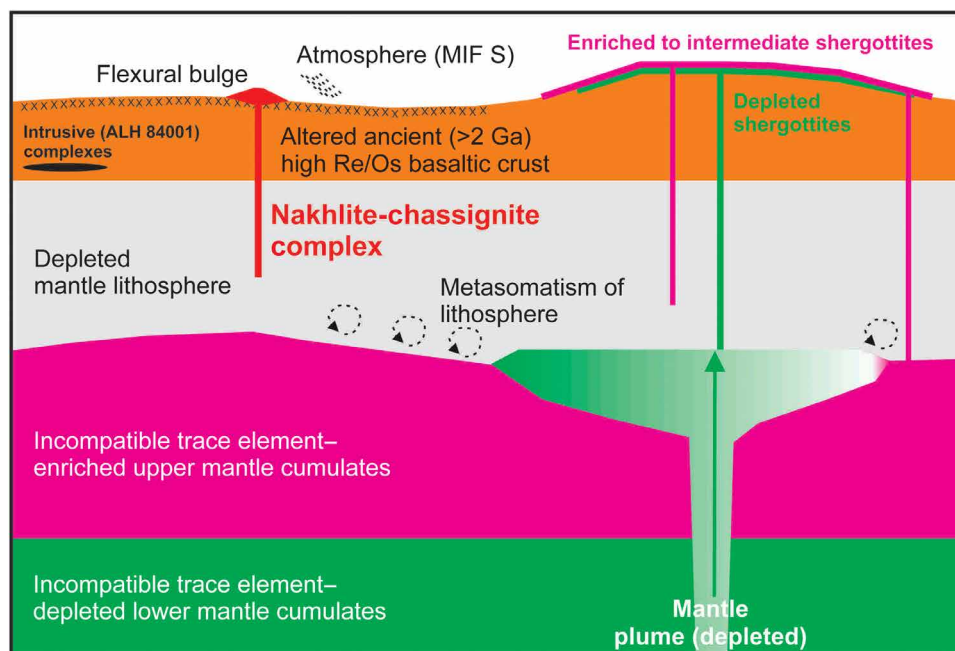


Fig. 5. Schematic illustration of relations of nakhlite-chassignites to other martian meteorites and major martian silicate reservoirs. Shown is the relationship of the flexural bulge due to loading of Tharsis on the lithosphere (16). Impingement by underlying plumes and small-scale melting at the lithosphere-asthenosphere boundary of Mars likely engenders mantle metasomatism, and this feature along with melting of ITE-enriched upper mantle cumulates likely explains enriched shergottites. Depleted shergottites require ITE-depleted sources and are likely fed from mantle plumes within Mars. Enriched and depleted shergottites could originate from the same regions on Mars or from distinct volcanic edifices. Nakhrites and chassignites were emplaced into older, altered, and enriched crust that did not experience noticeable impact contamination, like NWA 7034/7533. ALH 84001 is likely an intrusive cumulate of the old martian crust. MIF S refers to atmospheric that interacted with martian surface reservoirs.

the acid using CCl_4 and then back-extracted into HBr , before purification by microdistillation. Rhenium and the other HSE were recovered and purified from the residual solutions using standard anion exchange separation techniques (47). Isotopic compositions of Os were measured in negative-ion mode using a Thermo Fisher Scientific Triton thermal ionization mass spectrometer in peak-jumping mode on the secondary electron multiplier. Rhenium, Pd, Pt, Ru, and Ir were measured using a Cetac Aridus II desolvating nebuliser coupled to a Thermo Fisher Scientific iCAP Qc ICP-MS. Offline corrections for Os involved an oxide correction, an iterative fractionation correction using $^{192}\text{Os}/^{188}\text{Os} = 3.08271$ and assuming the exponential law, a ^{190}Os spike subtraction, and an Os blank subtraction. Precision for $^{187}\text{Os}/^{188}\text{Os}$, determined by repeated measurement of a 35-pg University of Maryland, College Park, Johnson-Matthey standard solution, was better than $\pm 0.2\%$ (2 SD; 0.11381 ± 12 ; $n = 12$). Rhenium, Ir, Pt, Pd, and Ru isotopic ratios for sample solutions were corrected for mass fractionation using the deviation of the standard average run on the day over the natural ratio for the element. External reproducibility for HSE analyses was better than 0.5% for 0.5-part-per-billion solutions, and all reported values are blank-corrected. The total procedural blanks ($n = 3$) run with the samples gave $^{187}\text{Os}/^{188}\text{Os} = 0.150 \pm 0.012$, with quantities (in picograms) of 2.5 (Re), 27 (Pd), 3.1 (Pt), 16 (Ru), 0.3 (Ir), and 0.3 (Os). Blanks contributions are listed in table S3 and resulted in negligible corrections for most elements within samples (<5%), unless noted in the table.

During the analytical campaign, the terrestrial basalt reference materials BHVO-2 and BCR-2 were analyzed, along with the in-house picritic reference sample 9C-TEN-05. These data have been previously reported (48) and are consistent with prior work (29).

Average reproducibility for BHVO-2 for $^{187}\text{Os}/^{188}\text{Os}$ is $\sim 3\%$ relative standard deviation (RSD%), with abundance reproducibility of 4 RSD% for Re and ~ 20 to 60 RSD% for Pd, Pt, Ru, Ir, and Os. This reproducibility demonstrates that absolute abundance variability can be considerable in some basaltic lava flows. Some of the variability of HSE abundances observed in nakhlite and chassignite powder aliquots must also reflect inhomogeneous distribution of HSE-rich phases (nuggeting) within the rocks from which they were derived.

Supplementary Materials

This PDF file includes:

Information on modeling in Figure 1
Figs. S1 to S3
Legends for tables S1 to S5
References

Other Supplementary Material for this manuscript includes the following:

Tables S1 to S5

REFERENCES AND NOTES

- H. Y. McSween Jr., Petrology on Mars. *Am. Mineral.* **100**, 2380–2395 (2015).
- T. J. Lapen, M. Richter, A. D. Brandon, V. Debaille, B. L. Beard, J. T. Shafer, A. H. Peslier, A younger age for ALH84001 and its geochemical link to shergottite sources in Mars. *Science* **328**, 347–351 (2010).
- L. C. Bouvier, M. M. Costa, J. N. Connelly, N. K. Jensen, D. Wielandt, M. Storey, A. A. Nemchin, M. J. Whitehouse, J. F. Snape, J. J. Bellucci, Evidence for extremely rapid magma ocean crystallization and crust formation on Mars. *Nature* **558**, 586–589 (2018).
- A. Udry, G. H. Howarth, C. D. K. Herd, J. M. D. Day, T. Lapen, J. Filiberto, What martian meteorites reveal about the interior and surface of Mars. *J. Geophys. Res. Planets* **125**, e2020JE006523 (2020).

5. N. Dauphas, A. Pourmand, Hf–W–Th evidence for rapid growth of Mars and its status as a planetary embryo. *Nature* **473**, 489–492 (2011).
6. V. Debaille, A. D. Brandon, Q. Z. Yin, B. Jacobsen, Coupled ^{142}Nd – ^{143}Nd evidence for a protracted magma ocean in Mars. *Nature* **450**, 525–528 (2007).
7. Z. Deng, F. Moynier, J. Villeneuve, N. K. Jensen, D. Liu, P. Cartigny, T. Mikouchi, J. Siebert, A. Agranier, M. Chaussidon, M. Bizzarro, Early oxidation of the martian crust triggered by impacts. *Sci. Adv.* **6**, eabc4941 (2020).
8. J. W. Valley, J. M. Eiler, C. M. Graham, E. K. Gibson, C. S. Romanek, E. M. Stolper, Low-temperature carbonate concretions in the Martian meteorite ALH84001: Evidence from stable isotopes and mineralogy. *Science* **275**, 1633–1638 (1997).
9. H. B. Franz, S.-T. Kim, J. Farquhar, J. M. D. Day, R. C. Economos, K. D. McKeegan, A. K. Schmitt, A. J. Irving, J. Hoek, J. Dottin, isotopic links between atmospheric chemistry and the deep sulphur cycle on Mars. *Nature* **508**, 364–368 (2014).
10. J. J. Barnes, F. M. McCubbin, A. R. Santos, J. M. D. Day, J. W. Boyce, S. P. Schwensen, U. Ott, I. A. Franchi, S. Messenger, M. Anand, C. B. Agee, Multiple early-formed water reservoirs in the interior of Mars. *Nat. Geosci.* **13**, 260–264 (2020).
11. D. S. McKay, E. K. Gibson Jr., K. L. Thomas-Keptra, H. Vali, C. S. Romanek, S. J. Clemett, X. D. Chilliier, C. R. Maechling, R. N. Zare, Search for past life on Mars: Possible relic biogenic activity in Martian meteorite ALH84001. *Science* **273**, 924–930 (1996).
12. A. H. Treiman, The nakhlite meteorites: Augite-rich igneous rocks from Mars. *Geochemistry* **65**, 203–270 (2005).
13. R. J. Floran, M. Prinz, P. F. Hlava, K. Keil, C. E. Nehru, J. R. Hinthorne, The Chassigny meteorite: A cumulate dunite with hydrous amphibole-bearing melt inclusions. *Geochim. Cosmochim. Acta* **42**, 1213–1229 (1978).
14. A. Udry, J. M. D. Day, 1.34 billion-year-old magmatism on Mars evaluated from the co-genetic nakhlite and chassignite meteorites. *Geochim. Cosmochim. Acta* **238**, 292–315 (2018).
15. B. E. Cohen, D. F. Mark, W. S. Cassata, M. R. Lee, T. Tomkinson, C. L. Smith, Taking the pulse of Mars via dating of a plume-fed volcano. *Nat. Commun.* **8**, 640 (2017).
16. J. M. D. Day, K. T. Tait, A. Udry, F. Moynier, Y. Liu, C. R. Neal, Martian magmatism from plume metasomatized mantle. *Nat. Commun.* **9**, 4799 (2018).
17. M. Wadhwa, G. Crozaz, Trace and minor elements in minerals of nakhlites and Chassigny: Clues to their petrogenesis. *Geochim. Cosmochim. Acta* **59**, 3629–3645 (1995).
18. A. H. Treiman, A petrographic history of Martian meteorite ALH84001: Two shocks and an ancient age. *Meteoritics* **30**, 294–302 (1995).
19. C. B. Agee, N. V. Wilson, F. M. McCubbin, K. Ziegler, V. J. Polyak, Z. D. Sharp, Y. Asmerom, M. H. Nunn, R. Shaheen, M. H. Thieme, A. Steele, Unique meteorite from early Amazonian Mars: Water-rich basaltic breccia Northwest Africa 7034. *Science* **339**, 780–785 (2013).
20. A. D. Brandon, R. J. Walker, J. W. Morgan, G. G. Goles, Re–Os isotopic evidence for early differentiation of the Martian mantle. *Geochim. Cosmochim. Acta* **64**, 4083–4095 (2000).
21. J. H. Jones, C. R. Neal, J. C. Ely, Signatures of the highly siderophile elements in the SNC meteorites and Mars: A review and petrologic synthesis. *Chem. Geol.* **196**, 5–25 (2003).
22. C. W. Dale, K. W. Burton, R. C. Greenwood, A. Gannoun, J. Wade, B. J. Wood, D. G. Pearson, Late accretion on the earliest planetesimals revealed by the highly siderophile elements. *Science* **336**, 72–75 (2012).
23. N. Mari, A. J. V. Riches, L. J. Hallis, Y. Marrocchi, J. Villeneuve, P. Gleissner, H. Becker, M. R. Lee, Syneruptive incorporation of martian surface sulphur in the nakhlite lava flows revealed by S and Os isotopes and highly siderophile elements: Implication for mantle sources in Mars. *Geochim. Cosmochim. Acta* **266**, 416–434 (2019).
24. S. Goderis, A. D. Brandon, B. Mayer, M. Humayun, Ancient impactor components preserved and reworked in martian regolith breccia Northwest Africa 7034. *Geochim. Cosmochim. Acta* **191**, 203–215 (2016).
25. S. R. Ramsey, A. M. Ostwald, A. Udry, E. O’Neal, J. M. D. Day, Z. Wilbur, J. J. Barnes, S. Griffin, Northwest Africa 13669, a re-equilibrated nakhlite from a previously unsampled portion of the nakhlite igneous complex. *Meteorit. Planet. Sci.* **59**, 134–170 (2024).
26. J. M. D. Day, Hotspot volcanism and highly siderophile elements. *Chem. Geol.* **341**, 50–74 (2013).
27. B. J. Peters, J. M. D. Day, L. A. Taylor, Early mantle heterogeneities in the Réunion hotspot source inferred from highly siderophile elements in cumulate xenoliths. *Earth Planet. Sci. Lett.* **448**, 150–160 (2016).
28. J. M. D. Day, R. J. Walker, O. B. James, I. S. Puchtel, Osmium isotope and highly siderophile element systematics of the lunar crust. *Earth Planet. Sci. Lett.* **289**, 595–605 (2010).
29. J. M. D. Day, A. D. Brandon, R. J. Walker, Highly siderophile elements in Earth, Mars, the Moon, and asteroids. *Rev. Mineral. Geochem.* **81**, 161–238 (2016).
30. F. M. McCubbin, S. M. Elardo, C. K. Shearer Jr., A. Smirnov, E. H. Hauri, D. S. Draper, A petrogenetic model for the comagmatic origin of chassignites and nakhlites: Inferences from chlorine-rich minerals, petrology, and geochemistry. *Meteorit. Planet. Sci.* **48**, 819–853 (2013).
31. M. Humayun, S. Yang, A. J. Irving, R. H. Hewins, B. Zanda, K. Righter, A. H. Peslier, “Tin abundances require that chassignites originated from multiple magmatic bodies distinct from nakhlites” in *Lunar and Planetary Science Conference* (No. JSC-E-DAA-TN77055, NASA, 2020).
32. K. T. Tait, J. M. D. Day, Chondritic late accretion to Mars and the nature of shergottite reservoirs. *Earth Planet. Sci. Lett.* **494**, 99–108 (2018).
33. J. Filiberto, Experimental constraints on the parental liquid of the Chassigny meteorite: A possible link between the Chassigny meteorite and a Martian Gusev basalt. *Geochim. Cosmochim. Acta* **72**, 690–701 (2008).
34. R. P. Harvey, H. Y. McSween Jr., Petrogenesis of the nakhlite meteorites: Evidence from cumulate mineral zoning. *Geochim. Cosmochim. Acta* **56**, 1655–1663 (1992).
35. K. R. Stockstill, H. Y. McSween Jr., R. J. Bodnar, Melt inclusions in augite of the Nakhlite Martian meteorite: Evidence for basaltic parental melt. *Meteorit. Planet. Sci.* **40**, 377–396 (2005).
36. V. Sautter, M. J. Toplis, J. P. Lorand, M. Macri, Melt inclusions in augite from the nakhlite meteorites: A reassessment of nakhlite parental melt and implications for petrogenesis. *Meteorit. Planet. Sci.* **47**, 330–344 (2012).
37. J. M. Brennan, N. R. Bennett, Z. Zajac, Experimental results on fractionation of the highly siderophile elements (HSE) at variable pressures and temperatures during planetary and magmatic differentiation. *Rev. Mineral. Geochem.* **81**, 1–87 (2016).
38. M. Paquet, J. M. D. Day, A. Udry, R. Hattingh, B. Kumler, R. R. Rahbi, K. T. Tait, C. R. Neal, Highly siderophile elements in shergottite sulfides and the sulfur content of the martian mantle. *Geochim. Cosmochim. Acta* **293**, 379–398 (2021).
39. J. Farquhar, S. T. Kim, A. Masterson, Implications for sulfur isotopes of the Nakhlite meteorite for the origin of sulfate on Mars. *Earth Planet. Sci. Lett.* **264**, 1–8 (2007).
40. J. W. Dottin, J. Labidi, J. Farquhar, P. Piccoli, M. C. Liu, K. D. McKeegan, Evidence for oxidation at the base of the nakhlite pile by reduction of sulfate salts at the time of lava emplacement. *Geochim. Cosmochim. Acta* **239**, 186–197 (2018).
41. J. M. D. Day, L. A. Taylor, C. Floss, H. Y. McSween Jr., Petrology and chemistry of MIL 03346 and its significance in understanding the petrogenesis of nakhlites on Mars. *Meteorit. Planet. Sci.* **41**, 581–606 (2006).
42. A. Udry, H. Y. McSween Jr., P. Lecumberri-Sanchez, R. J. Bodnar, Paired nakhlites MIL 090030, 090032, 090136, and 03346: Insights into the Miller Range parent meteorite. *Meteorit. Planet. Sci.* **47**, 1575–1589 (2012).
43. A. D. Brandon, I. S. Puchtel, R. J. Walker, J. M. D. Day, A. J. Irving, L. A. Taylor, Evolution of the martian mantle inferred from the ^{187}Re – ^{187}Os isotope and highly siderophile element abundance systematics of shergottite meteorites. *Geochim. Cosmochim. Acta* **76**, 206–235 (2012).
44. C. D. Herd, E. L. Walton, C. B. Agee, N. Muttik, K. Ziegler, C. K. Shearer, A. S. Bell, A. R. Santos, P. V. Burger, J. I. Simon, M. J. Tappa, The Northwest Africa 8159 martian meteorite: Expanding the martian sample suite to the early Amazonian. *Geochim. Cosmochim. Acta* **218**, 1–26 (2017).
45. T. J. Lapen, M. Righter, R. Andreasen, A. J. Irving, A. M. Satkoski, B. L. Beard, K. Nishiizumi, A. T. Jull, M. W. Caffee, Two billion years of magmatism recorded from a single Mars meteorite ejection site. *Sci. Adv.* **3**, e1600922 (2017).
46. J. A. Barrat, P. La Bachèry, La Réunion Island dunites as analogs of the Martian chassignites: Tracking trapped melts with incompatible trace elements. *Lithos* **344–345**, 452–463 (2019).
47. J. M. D. Day, C. L. Waters, B. F. Schaefer, R. J. Walker, S. Turner, Use of hydrofluoric acid desilicification in the determination of highly siderophile element abundances and Re–Pt–Os isotope systematics in mafic-ultramafic rocks. *Geostand. Geoanal. Res.* **40**, 49–65 (2016).
48. J. M. D. Day, K. L. Nutt, B. Mendenhall, B. J. Peters, Temporally variable crustal contributions to primitive mantle-derived Columbia River Basalt Group magmas. *Chem. Geol.* **572**, 120197 (2021).
49. A. E. Ringwood, Special papers-apollo 11 symposium: Petrogenesis of apollo 11 basalts and implications for lunar origin. *J. Geophys. Res.* **75**, 6453–6479 (1970).
50. S. B. Shirey, R. J. Walker, The Re–Os ISOTOPE system in cosmochemistry and high-temperature geochemistry. *Annu. Rev. Earth Planet. Sci.* **26**, 423–500 (1998).
51. J. P. Greenwood, L. R. Riciputi, H. Y. McSween Jr., L. A. Taylor, Modified sulfur isotopic compositions of sulfides in the nakhlites and Chassigny. *Geochim. Cosmochim. Acta* **64**, 1121–1131 (2000).

Acknowledgments: We are grateful to E. Pringle for assistance with sample preparation and analysis in the early phases of this project. Examined meteorites were sourced from the NASA Meteorite Working Group; the NIPR; the Smithsonian Institution of Washington; University of New Mexico Institute of Meteoritics; and the Natural History Museum, London; as well as from private dealers (M. Ouzillou, L. Labenne, and G. Hupé). These sources are acknowledged.

Funding: This work was supported by the NASA Solar Systems Workings (80NSSC21K0159) and Emerging Worlds program (80NSSC19K0932). **Author contributions:** J.M.D.D.: Writing—original draft, conceptualization, investigation, writing—review and editing, methodology, resources, funding acquisition, data curation, validation, supervision, formal analysis, project administration, and visualization. M.P.: Writing—original draft, conceptualization, writing—review and editing, and validation. A.U.: Writing—original draft, investigation, writing—review and editing, and resources. F.M.: Writing—review and editing. **Competing interests:** The authors declare that they have no competing interests. **Data and materials availability:** All data needed to evaluate the conclusions in the paper are present in the paper and/or the Supplementary Materials.

Submitted 10 January 2024
 Accepted 25 April 2024
 Published 31 May 2024
 10.1126/sciadv.adn9830